EGU2017-7459

# The assessment of different production methods for hydrate bearing sediments – results from small and large scale experiments

Judith M. Schicks, Katja Heeschen, Erik Spangenberg, Manja Luzi-Helbing, Bettina Beeskow-Strauch, Mike Priegnitz, Ronny Giese , Sven Abendroth, Jan Thaler
GFZ German Research Centre for Geosciences, Geochemistry, Potsdam, Germany (schick@gfz-potsdam.de)

## Introduction:

Natural gas hydrates occur at all active and passive continental margins, in permafrost regions, and deep lakes. Since they are supposed to contain enormous amounts of $CH_4$, gas hydrates are discussed as an energy resource.

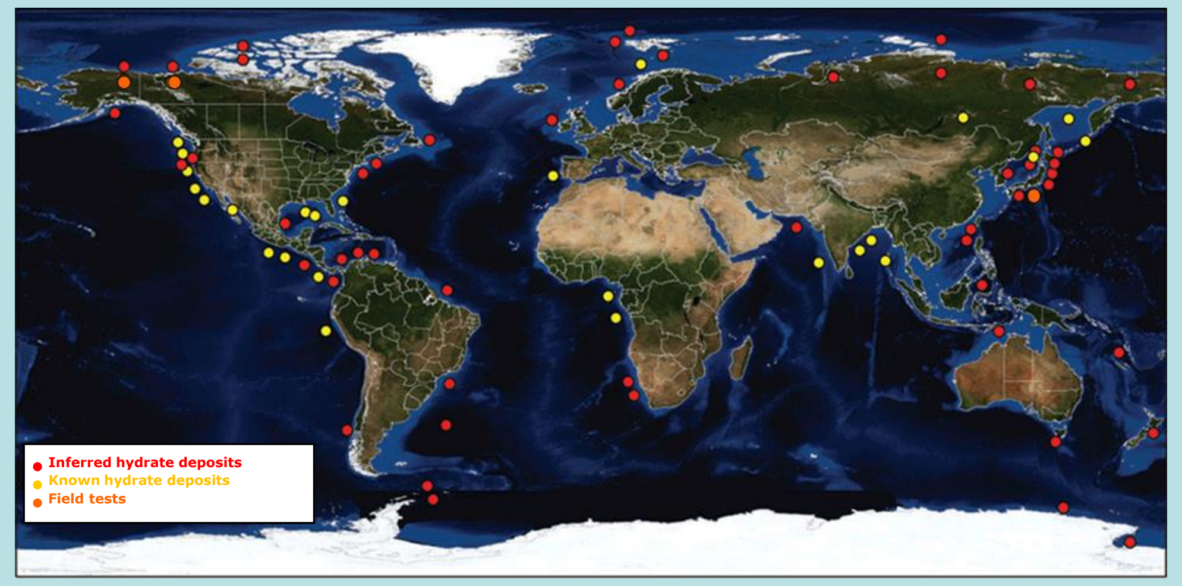

*Figure 1: Inferred and known hydrate deposits and field test locations.*

In general, three different methods can be used for the production of gas from natural gas hydrate deposits:

- thermal stimulation – increasing the reservoir temperature above the equilibrium temperature at given pressure
- depressurization – reducing the bottom hole pressure below the equilibrium pressure at given temperature
- chemical stimulation – changing the chemical environment by injection of salt, $CO_2$ or $CO_2$-$N_2$ mixtures.

All three methods have been tested in the field (see orange dots in Figure 1):

- thermal stimulation in Mallik (Northwest territories, Canada 2001/2001),
- depressurization in Mallik (2007/2008) and Nankai Trough (Japan, 2012/2013), and
- chemical stimulation by injection of a $CO_2$-$N_2$ mixture at Prudhoe Bay (Alaska North Slope, USA 2011/2012).

## Methods:

Raman spectroscopy, X-ray diffraction, microscopic observation, gas chromatography, and electrical resistivity measurements (ERT) were used to understand the processes occurring during the production of methane at different scales (400 µl to 425 l).

*in situ* Raman spectroscopy and X-ray diffraction

- cell volume ~ 400 µl /250 µl
- max. pressure 10 MPa/4MPa
- temperature range 248 K < T < 353 K
- gas flow: 1 ml/min

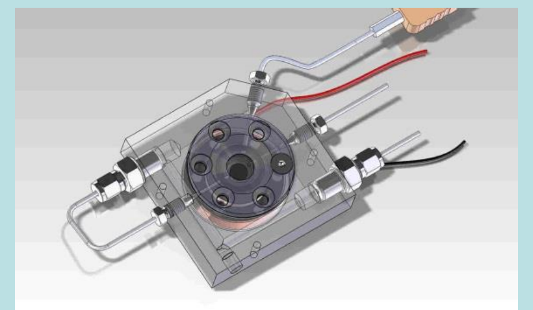

*Figure 2: Sketch of the pressure cell.*

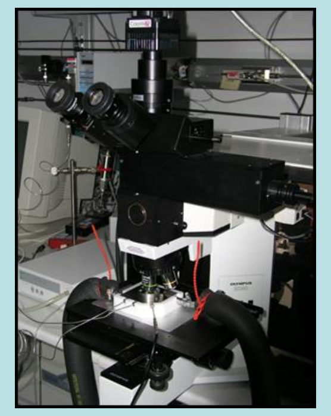

*Figure 3: Pressure cell mounted to the confocal microscope of the Raman spectrometer.*

tempered pressure vessels

- cell volume ~ 537 ml
- max. pressure 15 MPa
- min. temperature 253 K

*Figure 4: pressure vessels equipped with p-sensor stored in cooling box.*

*LArge Reservoir Simulator LARS*

- total volume 425 l
- sample volume 210 l
- max. pressure 250 MPa
- equipped with numerous temperature and pressure sensors + ERT

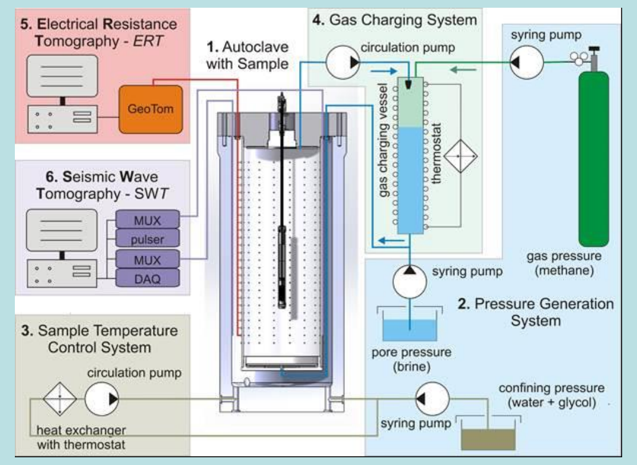

*Figure 5: 1) Temperature controlled pressure vessel with sediment sample 2) Pressure generation system with pumps for confining pressure and pore fluid pressure pumps 3) Temperature control system for the pressure vessel with chiller, heat exchanger and circulation pump for the confining pressure fluid 4) Temperature controlled gas charging pressure vessel with pore water circulation pump 5) Electrical resistivity tomography system 6) Seismic wave tomography system.*

## Results:

Within the SUGAR project started at 2008 we developed and tested the three different production methods (depressurization, thermal and chemical stimulation). We studied the processes inducing the dissociation of gas hydrates and the release of $CH_4$ on a molecular and up to a pilot plant scale.

### Thermal stimulation

This method was tested in a field test in the framework of the Mallik Scientific Drilling Project in the Northwest Territories in the Canadian Arctic in 2001/2002. During the World's first gas production test a hot fluid was pumped through about 600 m of permafrost into depths of 900–1100 m where the hydrate-bearing sediment occurred. About 470 $m^3$ of $CH_4$ were produced within 123.7 hours (Hancock et al. 2005).

The generation of heat within the hydrate bearing layer is probably more efficient. Therefore we developed a counter-current heat-exchange reactor for the thermal stimulation via *in situ* combustion.

The catalytic oxidation of $CH_4$ (flameless!) is an exothermic reaction. The heat generated by this reaction is used for the dissociation of the hydrate (Schicks et al. 2011a).

Catalytic oxidation of $CH_4$:

$$CH_4 + 2\,O_2 \rightarrow CO_2 + 2\,H_2O \qquad \Delta H = -802.7 \text{ kJ/mol}$$

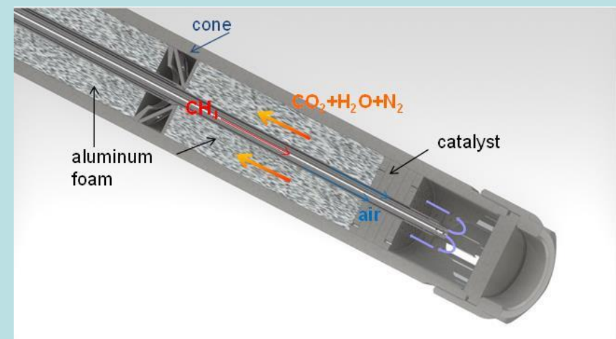

*Figure 6: Technical sketch of the counter-current heat-exchange reactor.*

*Figure 7: Catalyst (Pd on $Al_2O_3$). The catalyst has to be preheated with the combustion of $H_2$.*

Several experiments were conducted in LARS with different hydrate saturations (40-80%) to test the efficiency of production $CH_4$ from hydrate bearing sediments using *in situ* combustion (Schicks et al. 2013). The method seems to be quite promising: only 15% of the produced $CH_4$ was needed to generate enough heat for the dissociation of the hydrates in LARS.

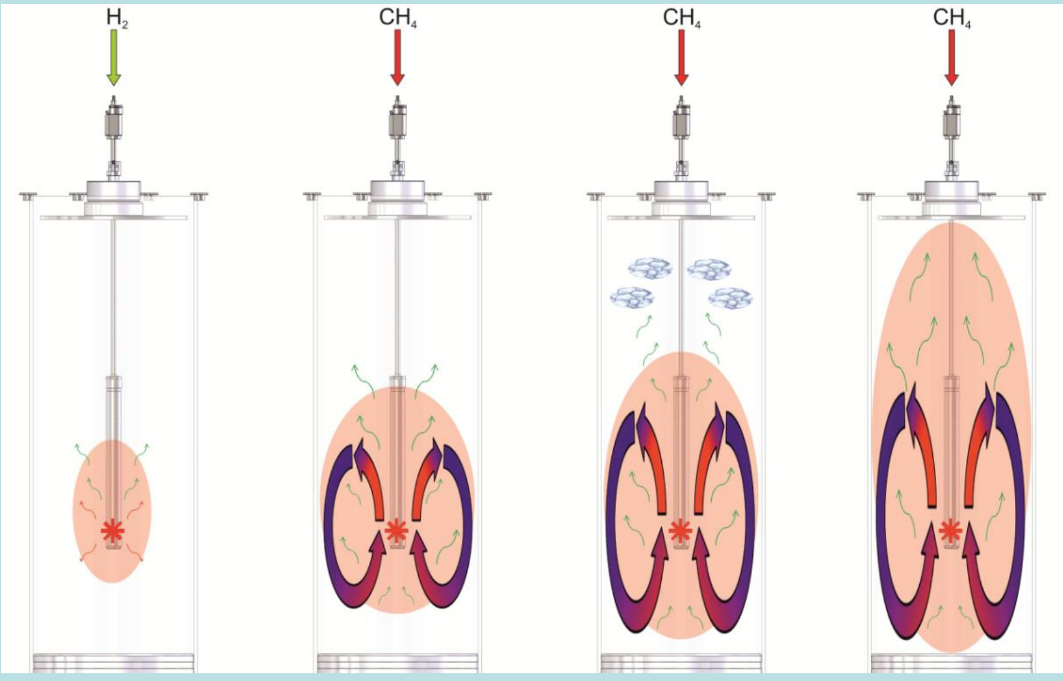

*Figure 8. (a) During the ignition of the catalyst using $H_2$ heat was already generated and induced hydrate dissociation in the vicinity of the reactor; (b) When the fuel was changed to $CH_4$ the temperature at the catalyst increased rapidly to 450 ° C. The generated heat induced a strong increase of the fluid temperature close to the reactor causing a convection process; (c) Since the released gas from dissociated hydrates migrated faster through the sediment than the heat front, secondary hydrates formed in the colder areas at the top of LARS; (d) After 12 h the temperatures in almost all areas of LARS were outside the stability field of $CH_4$ hydrate at given pressure (Schicks et al. 2013).*

### Depressurization

In 2007/2008 a depressurization test was obtained at Mallik. The initial hydrate saturation of the sediment below the permafrost was 80-90%.

Within 6.75 days 12,278 $m^3$ of gas and 66.9 $m^3$ of water were produced from gas hydrates via depressurization in three pressure stages: 7.1−5.0−4.2 MPa.

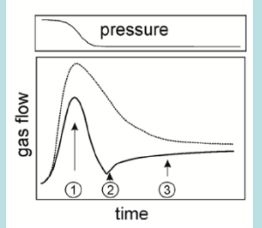

An unconventional gas flow was observed during field production test (see Figure 9 and Heeschen et al. 2016).

*Figure 9: Sketch of the hydraulic signal of classical (dotted line) and unconventional (solid line) reservoir response*

We simulated the Mallik depressurization field test in LARS to understand the transport behavior of gases and fluids. Experimental conditions were close to those at Mallik:

- two experiments (A + B)
- initial hydrate saturation 90%
- quartz sand
- initial pressure 11 MPa
- pressure stages 9.0−7.0−5.0−4.2(−3.0)

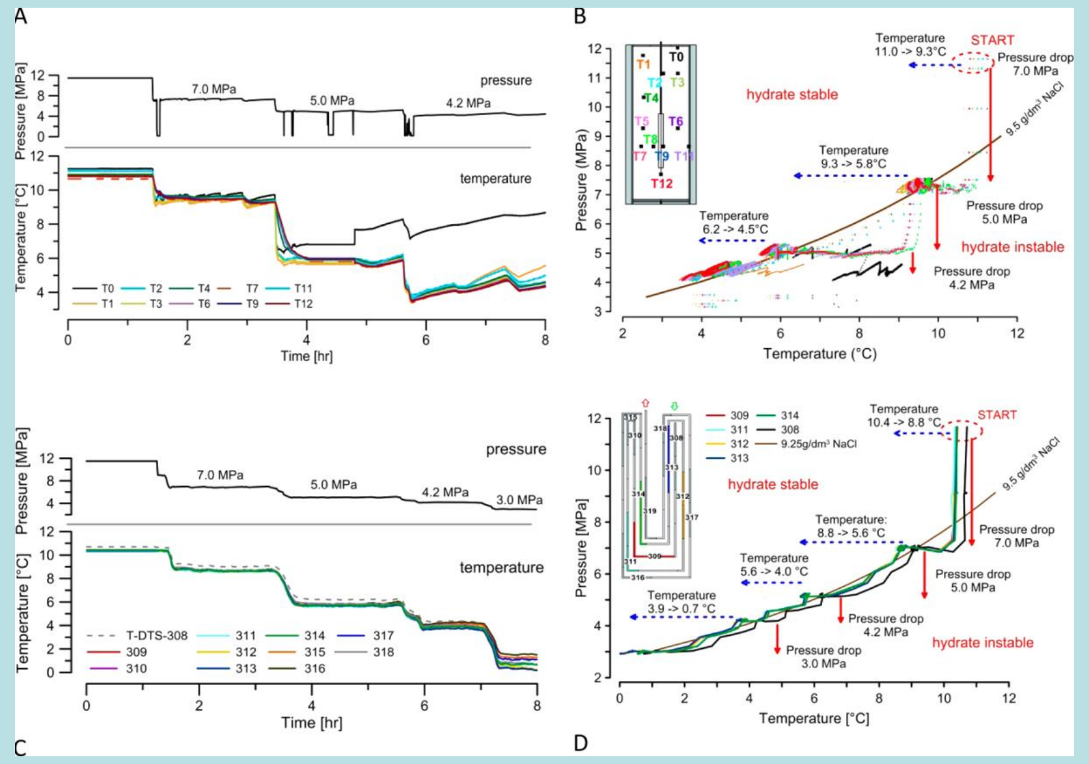

*Figure 10: (A) Progress of pressure (upper panel) and temperature (lower panel) during experiment A. (B) P−T paths as recorded during experiment A in comparison to calculated methane hydrate stability curves at 9.5 g/dm³ NaCl (using CSMGem software). Red arrows indicate the induced pressure steps. Dashed blue lines indicate accompanying average temperature changes. (C) Progress of pressure (upper panel) and temperature (lower panel) during experiment B with sensor distribution in Figure 3D. (D) P−T paths as recorded during experiment B (Heeschen et al. 2016).*

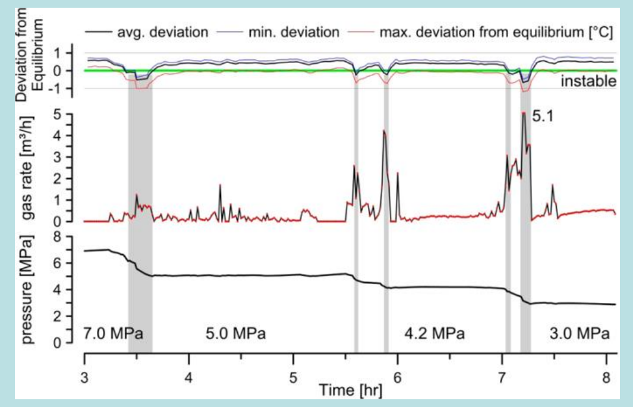

At the beginning of each pressure stage, gas hydrate was destabilized and large amounts of released gas form a continuous gas phase, leading to the observed gas surge.

*Figure 11: Deviations from the gas hydrate stability calculated by the subtraction of calculated data using CSMGem3 and those deduced from P−T measurements in LARS (upper panels), measured gas production rates (middle panels), and reservoir pressure (lower panel) over time in LARS during experiment B. (Heeschen et al. 2016).*

### Chemical stimulation

Changing the chemical environment of $CH_4$ hydrate via injection of $CO_2$ induces complex processes. We performed two experiments injecting warmed $CO_2$ into $CH_4$ hydrate bearing sediments on a macro scale in LARS (see poster EGU2017-13859: Heeschen et al.).

In a series of small scale experiments we investigated the „exchange" of hydrate-bonded $CH_4$ with $CO_2$ on a molecular scale with Raman spectroscopy and X-ray diffraction. Pure $CH_4$ hydrate as well as $CH_4$-$C_2H_6$ and $CH_4$-$C_3H_8$ hydrate was exposed to $CO_2$ (Schicks et al. 2011b).

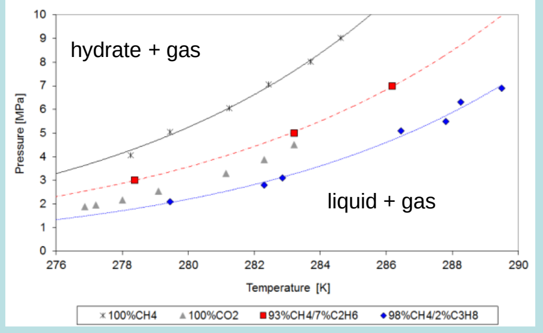

*Figure 12: Phase boundaries of hydrates formed from pure $CO_2$, pure $CH_4$ as well as mixed $CH_4$-$C_2H_6$ and $CH_4$-$C_3H_8$.*

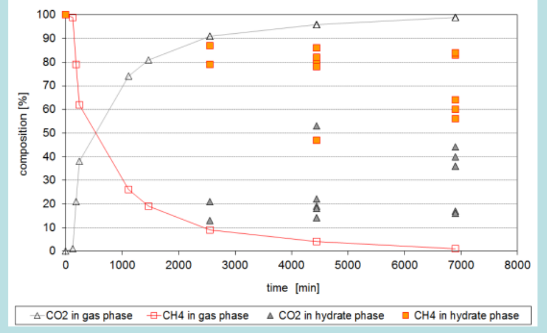

*Figure 13: Composition change of hydrate phase when pure $CH_4$ hydrate was exposed to $CO_2$ gas (based on Raman spectroscopy). Experimental conditions: p= 3.2 MPa, T= 274 K.*

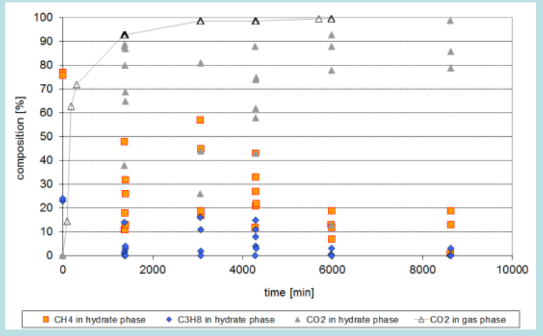

*Figure 14: Composition change of hydrate phase when mixed $CH_4$-$C_3H_8$ hydrate was exposed to $CO_2$ gas (based on Raman spectroscopy). Experimental conditions: p= 3.2 MPa, T= 274 K.*

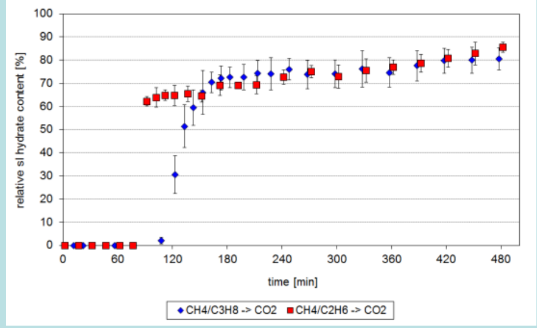

*Figure 15: PXRD data show structural changes versus time for $CH_4$-$C_2H_6$ mixed hydrate and the $CH_4$-$C_3H_8$ mixed hydrate into a structure I hydrate (when exposed to $CO_2$). Experimental conditions for $CH_4$-$C_2H_6$: p = 1.43 MPa, T = 267 K; $CH_4$-$C_3H_8$: p = 1.16 MPa, T = 267 K.*

A change of the hydrate composition from the initial $CH_4$ or $CH_4$-$C_3H_8$ hydrate to a mixed hydrate containing $CO_2$ besides $CH_4$ (and $C_3H_8$) could be proved with Raman spectroscopy. X-ray diffraction also indicate a change of the hydrate structure: The structure II mixed $CH_4$-$C_2H_6$ and $CH_4$-$C_3H_8$ hydrate transform into structure I mixed hydrates when exposed to $CO_2$. hydrate. All observed transformations are reversible when the hydrate phase is exposed to the initial gas phase.

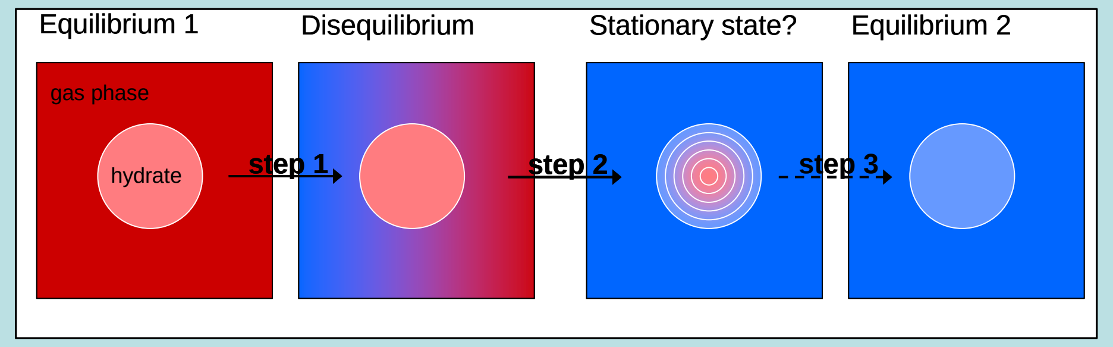

*Figure 16: Illustration of the conversion process in three steps. Starting point is equilibrium 1. With changing of gas phase the equilibrium state is disturbed (step 1) and decomposition/reformation occurs until a stationary state has reached (step 2). This stationary state will slowly develop to equilibrium 2 driven by the gradient in the chemical potential within the hydrate particle (step 3) (Schicks et al. 2011b).*

## Summary and Conclusions

Depressurization, thermal and chemical stimulation were tested as methods for the production of gas from natural gas hydrates. The aim of our experiments was the understanding of processes related to these method on a macro scale (e.g. transport behavior of gases and fluids) and on a molecular scale such as the exchange process of hydrate bonded $CH_4$ with $CO_2$.

Thermal stimulation:

- efficient *in situ* heat generation
- safe generation of heat using catalytic oxidation of $CH_4$
- heat transfer by conduction and convection
- limited gas production at the beginning of the experiments
  → possible re-formation of hydrates
- after 12 h all T-sensors indicate hydrates to be out of stability field
- 15% of the produced gas was needed for the generation of the necessary heat for hydrate dissociation

Depressurization:

- efficient method in sediments with high permeability
- transport processes strongly depend on reservoir/experimental conditions
- release of large amounts of gas when hydrate is out of stability field (gas surge)
- endothermic dissociation of gas hydrates initiates temperature decrease → stabilization of hydrate phase → discontinuation of gas production

Chemical stimulation ($CO_2$ injection):

- conversion of $CH_4$ hydrate to $CO_2$ hydrate is a slow process it is induced by the gradient of the chemical potential between the hydrate phase and the environmental gas phase
- the conversion process can be described as a rearrangement of molecules (partial decomposition and reformation process)
- the conversion rate depends on (equilibration) time, the surface area of the hydrate phase, and transport processes
- the conversion rate also depends on the concentration gradient of one component between the hydrate phase and the gas phase.
- the conversion of a $CH_4$ hydrate into a $CO_2$ rich hydrate is reversible when the hydrate is exposed to the initial gas phase.

Conclusions:

- depressurization is an efficient method for the production of $CH_4$ from hydrate bearing sediments with high permeability and sufficient heat transfer
- thermal stimulation using in situ combustion is probably an appropriate addition to enhance the efficiency of depressurization in areas with insufficient heat transfer
- compared to thermal stimulation and depressurization chemical stimulation via $CO_2$ injection is the most inefficient way to produce $CH_4$ from hydrate bearing sediments because the "exchange" of hydrate-bonded $CH_4$ with $CO_2$ is a very slow and incomplete reaction leading to the production of a gas mixture containing $CO_2$ and $CH_4$.

Acknowledgment: The German Federal Ministry for Economic Affairs and Energy and the Federal Ministry of Education and Research provided funding for this work through Research Grants 03SX320E and 03G0856C.

References:

S.H. Hancock, T:S. Collett, S.R. Dallimore, T. Satoh, T. Inoue, E. Huenges, J. Henninges, and B. Weatherill, Scientific Results from the Mallik 2002 Gas Hydrate Production Research Well Program, Mackenzie Delta, NWT, Canada, Geological Surves of Canada, 2005, Bulletin 585, 135.
K. U. Heeschen, S. Abendroth, M. Priegnitz, E. Spangenberg, J. Thaler, and J. M. Schicks, Energy & Fuels, 2016, 30, 6210−6219.
J. M. Schicks, E. Spangenberg, R. Giese, B. Steinhauer, J. Klump, M. Luzi, Energies, 2011a, 4, 151-172.
J. M. Schicks, M. Luzi, B. Beeskow-Strauch, Journal of Physical Chemistry A, 2011b, 115, 13324–13331.
J. M. Schicks, E. Spangenberg, R. Giese, M. Luzi-Helbing, M. Priegnitz, B. Beeskow-Strauch, Energies, 2013, 6, 3002-3016.

www.gfz-potsdam.de